

PNNL-34857

Mixed Oxygenate Conversion to Sustainable Aviation Fuel via Ketones Intermediate

September 2023

Karthikeyan Ramasamy
Mond Guo
Udishnu Sanyal
Laura Meyer

DISCLAIMER

This report was prepared as an account of work sponsored by an agency of the United States Government. Neither the United States Government nor any agency thereof, nor Battelle Memorial Institute, nor any of their employees, makes **any warranty, express or implied, or assumes any legal liability or responsibility for the accuracy, completeness, or usefulness of any information, apparatus, product, or process disclosed, or represents that its use would not infringe privately owned rights.** Reference herein to any specific commercial product, process, or service by trade name, trademark, manufacturer, or otherwise does not necessarily constitute or imply its endorsement, recommendation, or favoring by the United States Government or any agency thereof, or Battelle Memorial Institute. The views and opinions of authors expressed herein do not necessarily state or reflect those of the United States Government or any agency thereof.

PACIFIC NORTHWEST NATIONAL LABORATORY
operated by
BATTELLE
for the
UNITED STATES DEPARTMENT OF ENERGY
under Contract DE-AC05-76RL01830

Printed in the United States of America

Available to DOE and DOE contractors from
the Office of Scientific and Technical Information,
P.O. Box 62, Oak Ridge, TN 37831-0062
www.osti.gov
ph: (865) 576-8401
fox: (865) 576-5728
email: reports@osti.gov

Available to the public from the National Technical Information Service
5301 Shawnee Rd., Alexandria, VA 22312
ph: (800) 553-NTIS (6847)
or (703) 605-6000
email: info@ntis.gov
Online ordering: <http://www.ntis.gov>

0BMixed Oxygenate Conversion to Sustainable Aviation Fuel via Ketones Intermediate

Enter Subtitle Here (or delete)

September 2023

Karthikeyan Ramasamy
Mond Guo
Udishnu Sanyal
Laura Meyer

Prepared for
the U.S. Department of Energy
under Contract DE-AC05-76RL01830

Pacific Northwest National Laboratory
Richland, Washington 99354

Abstract

This report describes our effort in developing Pd based bimetallic catalysts during Tandem ketone condensation-hydrogenation reaction. We have synthesized a series of bimetallic catalysts containing equimolar amount of Pd with various other 3d, 4d and 5d transition and coinage metals. The activity of these bimetallic catalysts towards C=C and C=O hydrogenation was evaluated using mesityl oxide and 2-heptanone as model compounds. All these catalysts show much higher activity towards C=C hydrogenation compared to C=O hydrogenation at a given temperature and at different H₂ pressure, indicated the higher intrinsic activity of Pd based bimetallic catalysts towards C=C hydrogenation. Alloy catalysts with Pd and other 4d and 5d metals such as PdRu, PdRh, PdPt and PdIr shows higher activity towards both C=C and C=O hydrogenation compared to baseline Pd catalyst as well as alloy catalysts containing Pd and 3d transition metals. Among the different Pd-3d metal alloy catalysts, the activity of the bimetallic catalysts depends on alloying transition metals. Although, PdRu, PdRh, PdPt and PdIr catalysts shows very high activity towards C=O hydrogenation of 2-heptanone, the same catalysts didn't show any C=O hydrogenation when α,β -unsaturated carbonyl compound such as mesityl oxide was used as the model substrate. Based on these results, it is evident that Pd based bimetallic catalysts are very selective to the C=C hydrogenation and their activity could be tuned by the judicious choice of the alloying elements. Although alloying with Ru, Rh and Pt shows significant rate enhancement in case of C=C hydrogenation reaction, higher cost of those metals prevents their usage in industry as it significantly increases the cost of the catalyst. Considering all the factors, we have identified PdZn as one of promising alternative of Pd catalyst as it shows comparable activity towards C=C hydrogenation and reduces the activity for C=O hydrogenation. Based on the electrochemical CO stripping, we unambiguously established the weaker bonding CO on the PdZn surface compared to pristine Pd and highlight the benefits of its usage due to higher CO tolerance.

Acknowledgments

This research was supported by the Strategic Mission Investment, under the Laboratory Directed Research and Development (LDRD) Program at Pacific Northwest National Laboratory (PNNL). PNNL is a multi-program national laboratory operated for the U.S. Department of Energy (DOE) by Battelle Memorial Institute under Contract No. DE-AC05-76RL01830.

Contents

Abstract.....	ii
Acknowledgments.....	iii
Acronyms and Abbreviations.....	iv
1.0 Introduction	1
1.1 Research Design	2
2.0 Methods and Materials	3
3.0 Results and discussion.....	5
4.0 Conclusion	11
5.0 Reference.....	13

Figures

Figure 1. Overall reaction scheme that shows the conversion of lignocellulosic and other low carbon feedstocks to sustainable aviation fuel via ethanol intermediate.....	1
Figure 2. Different reaction pathways during the ketone condensation and hydrogenation reaction using 2-heptanone as the model ketone.....	2
Figure 3. Schematic representation of catalyst preparation and hydrogenation reaction performed in a high throughput stirred batch reactor.....	4
Figure 4. Powder XRD pattern of different Pd based bimetallic catalysts along with baseline Pd catalysts as well as support materials.....	5
Figure 5. (a) low and (b) high magnification TEM images of Pd/MgO-Al ₂ O ₃ catalyst. (c) BET surface area of MgO-Al ₂ O ₃ catalyst with and without Pd.....	6
Figure 6. Activity of Pd-based bimetallic catalysts towards MO conversion which yielded MIBK as the sole product. Reaction condition: 20 wt% MO, 40 °C, 45 psi H ₂	7
Figure 7. Activity of Pd-based bimetallic catalysts towards MO conversion at different hydrogen pressure. Reaction condition: 20 wt% MO, 40 °C, H ₂ pressure 45-270 psi.....	7
Figure 8. Activity of Pd-based bimetallic catalysts towards 2-heptanone hydrogenation. Reaction condition: 20 wt% MO, 40 °C, H ₂ pressure 45-270 psi.....	8

Figure 9. Activity of Pd-based bimetallic catalysts towards 2-heptanone hydrogenation at different hydrogen pressure. Reaction condition: 20 wt% MO, 40 °C, H ₂ pressure 45-270 psi.....	9
Figure 10. Comparison of activity among different Pd-based bimetallic catalysts during MO and 2-heptanone hydrogenation. Reaction condition: 20 wt% MO, 40 °C, H ₂ pressure 130 psi.....	10
Figure 11. (a) Electrochemical CO stripping spectrum of PdZn/C catalyst. (b) comparison of CO stripping peak among Pd and PdZn catalyst.....	11

1.0 Introduction

Renewable ethanol can be generated in large volumes from a variety of feedstocks across the globe. Today, ethanol production exceeds 30 billion gallons per year.¹ Given the variability in the feedstocks from which ethanol is derived and the diversity of local markets, the development of flexible and dynamic ethanol upgrading processes is crucial.² At the same time, these technologies are not intrinsically tied to bioethanol, as ethanol can be derived from a wide variety of sources, including cellulosic biomass, residual biomass, municipal solid waste (MSW), biogas, and flue gas. Many of these sources may potentially provide ethanol feedstocks at an even lower energy intensity and greenhouse gas footprint compared to corn ethanol (e.g., cellulosic biomass, MSW, flue gas). PNNL's SAF technology, via ketones intermediate, enables a novel approach to convert ethanol generated from lignocellulosic and other low-cost feedstocks to SAF that is rich in cycloalkanes and exceeds carbon emission reduction goals.^{2,3} Unique highlights of the process include:

- Complete single-pass conversion to desired products for all unit operations greatly simplifies process complexity.
- All hydrogen that is required to fully saturate and finish the SAF in this process is generated internally, eliminating the need for an external hydrogen source.
- Robust catalyst is highly tolerant to water and other oxygenate impurities, reducing feedstock cleanup requirements.
- Control over iso-paraffins and cycloalkanes content in the final fuel product composition improves flexibility in optimizing for desired SAF properties.
- In addition to being suitable for large-scale standalone plants, the characteristics of the process make it uniquely applicable for a bolt-on modular approach.

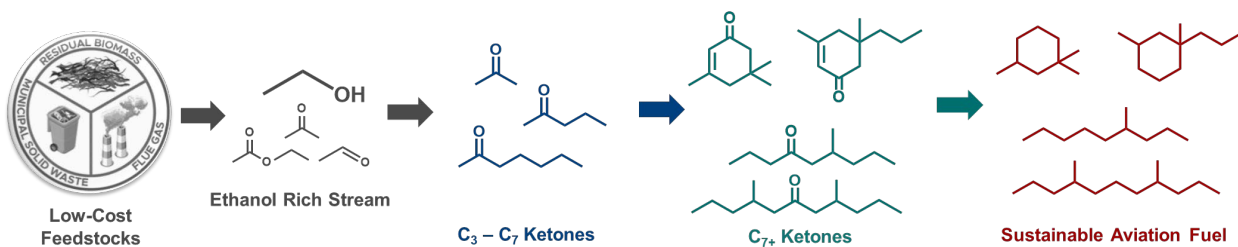


Figure 1. Overall reaction scheme that shows the conversion of lignocellulosic and other low carbon feedstocks to sustainable aviation fuel from ethanol via ketone intermediate.

Figure 1 shows the overall conversion process in which bioethanol could be obtained from variety of different low carbon feedstocks such as lignocellulosic or municipal solid waste (MSW). Ethanol thus obtained goes through three individual catalytic steps such as (i) ketone synthesis which produces C₃-C₇ methyl ketones, (ii) ketone condensation which produces a mixture of C₇+ linear and cyclic ketones and (iii) hydrodeoxygenation. We have recently demonstrated higher activity of Pd/ZnO-ZrO₂ catalyst for the efficient synthesis of methyl ketones. The higher stability of the catalyst was also demonstrated by continuous 2000 h time on stream performance.⁴ *In-situ* formation of PdZn alloy phase was attributed to the exceptional stability as it helps maintains dispersed Pd sites and prevent sintering the active sites. Thus, catalyst development for the ketone synthesis, and hydrogenation steps (commercially available Ni/C catalyst has been used in this step) are already matured and no further invention was needed. On the other hand, there still a significant opportunity to considerably improve the ketone condensation step. Our current unoptimized ketone condensation catalyst consist of Pd promoted MgO-Al₂O₃, which suffers from two drawbacks: 1) it requires regeneration for every 80-100 hours' time on stream due to the

catalyst deactivation from impurities such as carbon monoxide (CO) and 2) it can relatively unselective toward the desired C=C hydrogenation reaction versus unwanted C=O hydrogenation at relevant operating conditions. The specific goal of this study is to address both these issues by developing and demonstrating a durable and stable catalyst for the ketones condensation step that is highly selective toward C=C hydrogenation.

1.1 Research Design

During ketone condensation reaction, C₃₊ ketones undergo C-C coupling reaction via aldol condensation to generate α,β -unsaturated ketones. Selective hydrogenation of C=C moiety present in this α,β -unsaturated ketones is essential to prevent parallel Michael addition reaction that results in compounds with longer carbon chain not suitable for jet fuel. The large compounds formed during the reaction not only decrease the overall carbon yield of the process but also contribute to the deactivation of the catalyst. On the other hand, the metal catalyst (e.g., Pd) that are used to facilitate chemo selective hydrogenation of C=C are often prone to deactivation in presence of trace amounts of CO that are present as impurities in the ketone feedstock. The goal of this project is to develop bimetallic catalysts with improved activity towards selective C=C hydrogenation as well as tolerance towards CO impurities. We hypothesize that alloying different metals will provide an opportunity to tune the electronic natures of the metal catalysts which in turn modulates the interaction with corresponding adsorbates and facilitate the desired reaction pathways. Scheme 1 shows the different pathways during ketone condensation reaction and hydrogenation which shows the choice of the catalyst must activate C=C selectively otherwise C=O reduction of the initial ketones leads to undesired dead-end alcohol products that cannot be further converted to jet fuel.

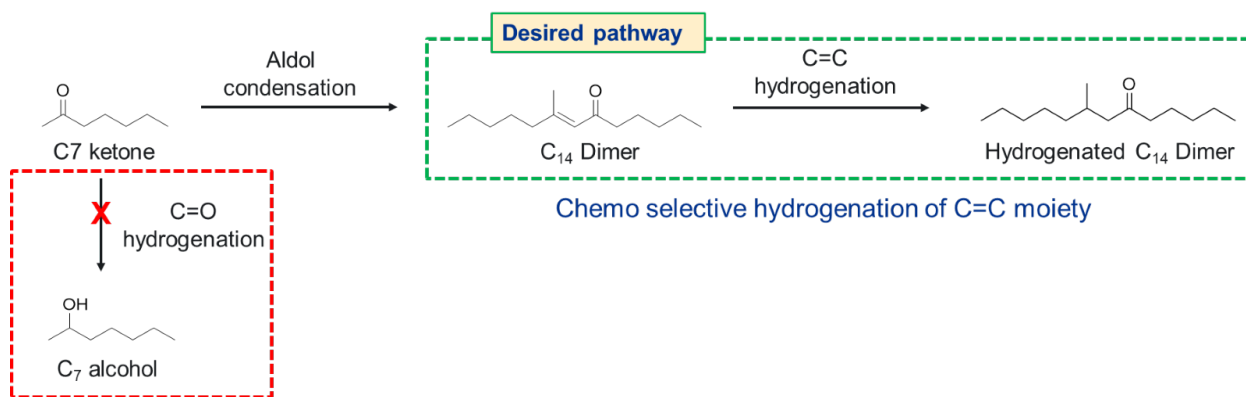


Figure 2. Different reaction pathways during the ketone condensation and hydrogenation reaction using 2-heptanone as the model ketone.

2.0 Methods and Materials

All the chemicals such as spinel magnesium alumina (3MgO: 7Al₂O₃, PURAL 30) was procured from Sasol. All the metal nitrate salts were purchased from sigma Aldrich and used as received.

Catalyst synthesis

Bimetallic Pd alloys were prepared by incipient wetness impregnation of an equimolar aqueous solution of Pd with salts of other transition metals (Mn, Fe, Co, Ni, Cu, Zn, Y, Ru, Rh, Ag, Ir, and Pt) on Pural support. The bimetallic catalysts were dried overnight at 90 °C in an oven and later transferred to a custom made 48 cell reactors capable of simultaneously studying the reactor. The bimetallic catalysts were first reduced in 5 vol. % H₂ in N₂ at 350 °C for 6 h using a ramp rate 2°C/min. The reduced catalyst was transferred to a glove box without exposing to air. References

Catalyst characterization

The composition of the bimetallic catalyst was analyzed using inductively coupled plasma-optical emission spectrometry (ICP-OES) on a Perkin Elmer Optima 7300DV instrument. Before ICP measurements, the bimetallic catalysts were digested in concentrated nitric acid in a sealed vessel using CEM MARS 6 microwave digestion unit. The crystal structure of the bimetallic catalysts was studied using a benchtop Rigaku MiniFlex 600 X-ray diffractometer equipped with a Cu K_α X-ray source (wavelength of 1.54 Å). To obtain X-ray diffraction (XRD) patterns, the bimetallic catalyst was placed on a glass sample holder and diffraction patterns were collected over the scattering angle range of 5° to 80°, with a scan rate of 0.1° min⁻¹ and a step size of 0.01°. The morphology and the particle size of the Pd catalysts were evaluated using transmission electron microscope (TEM). The textural properties of the bimetallic catalysts were analyzed using a Micromeritics ASAP 2020 porosimeter. Nitrogen (N₂) adsorption isotherms of the bimetallic catalysts were obtained at 77 K, and surface area and pore volume for each MOF were evaluated using Brunauer-Emmett-Teller theory.³

Selective hydrogenation reaction

Before evaluating the hydrogenation activity of the Pd-based catalysts, the bimetallic catalysts were weighed and distributed in glass vials in a custom 48-cell reactor. For the sake of accuracy, triplicates on each catalyst were studied, including bare support. 1.75 mL of 20 wt% of substrate in dodecane were pipetted into each vial. The different substrates that were used for hydrogenation reaction in this study were mesityl oxide (MO), methyl isobutyl ketone (MIBK), and 2-heptanone.

Electrochemical CO stripping experiment

Electrochemical CO stripping experiment was carried out in a rotating disc electrode (RDE). The catalyst ink was prepared by dispersing Pd/C or PdZn/C catalyst in presence of nafion. 3:1 vol% isopropanol and water were used as the solvent system for the ink preparation. Commercial sodium acetate-acetic acid buffer with pH 5.2 was used as the electrolyte during the experiment. Pretreatment of the catalyst was carried out by applying a suitable potential to ensure the reduction of the metallic phase. After pretreatment, CO was purged for 30 min followed by Ar purging to remove any dissolved CO in the electrolyte. Stripping experiment was carried out by running cyclic voltammetry with a potential range -0.3 V to 1 V vs Ag/AgCl using scan rate 20 mV/s.

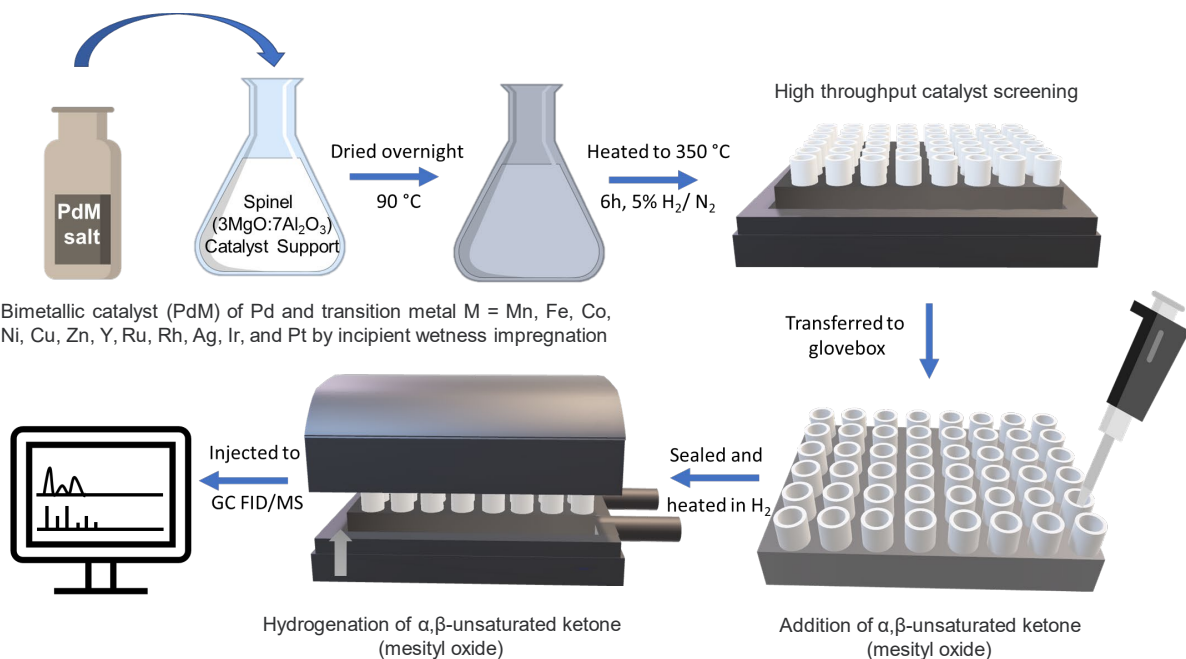


Figure 3. Schematic representation of catalyst preparation and hydrogenation reaction performed in a high throughput stirred batch reactor.

3.0 Results and discussion

All the different Pd based bimetallic catalysts prepared herein were characterized by powder XRD pattern to investigate the alloy formation. Figure 4 shows the powder XRD pattern of these catalysts which shows shift of Pd (111) peaks either to lower or higher 2θ value depending on the alloying metals which suggest the bimetallic alloy formation. The (111) peak shifts to lower 2θ value if the size of the alloying elements are larger than Pd which causes the expansion of the Pd lattice. On the other hand, if the alloying elements are smaller than Pd then shift towards higher 2θ value was obtained due to the contraction of lattice. Powder XRD of the bimetallic catalysts were also compared with baseline Pd catalysts and the support itself. Broad peaks associated with most of the catalysts were attributed to the smaller size of the crystallites as well as strong interaction between metal and support phase.

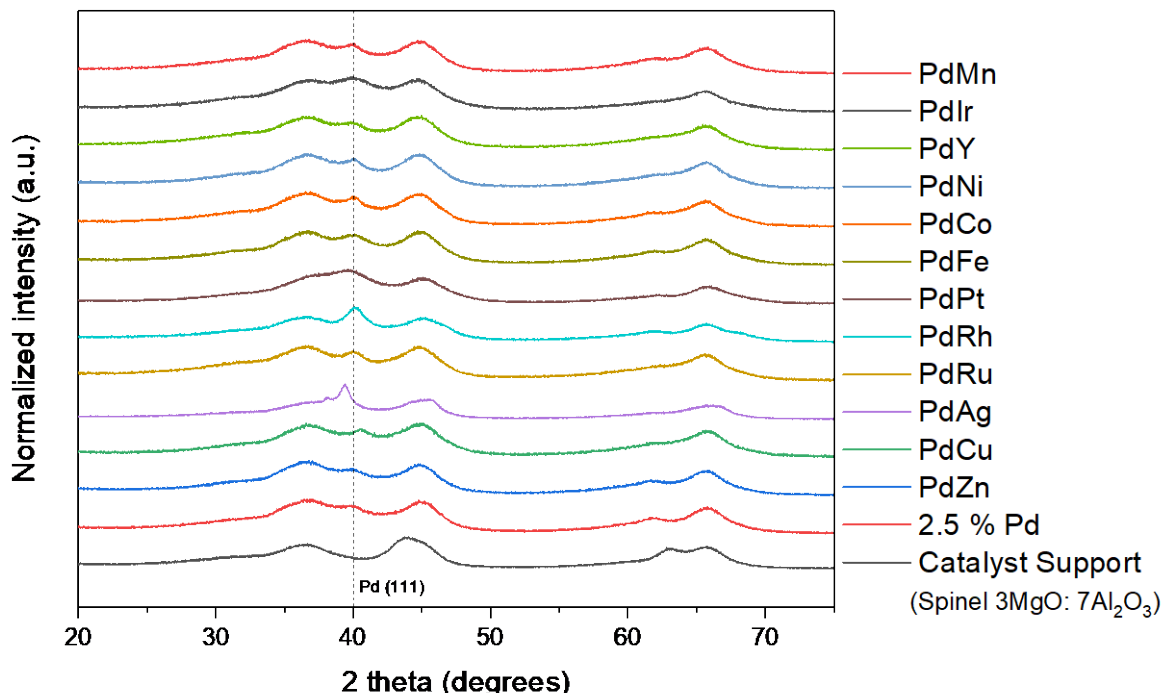


Figure 4. Powder XRD pattern of different Pd based bimetallic catalysts along with baseline Pd catalysts as well as support materials.

The microscopic characterization of the baseline Pd catalysts are shown in Figure 5. Figure 5a and 5b shows low and high magnification Pd/MgO-Al₂O₃ catalyst respectively. The average particle size calculated for these images are ~ 3 nm. The physical structure support materials were also investigated to understand the effect of deposition of metallic phase. Figure 5c shows the BET surface area of MgO-Al₂O₃ support with and without Pd metal. BET surface area of spinel MgO-Al₂O₃ was determined as 217 m²/g whereas the same was obtained as 198 m²/g after depositing of Pd. The minor decrease in surface area with Pd catalyst is attributed to the presence of Pd particles in the pore.

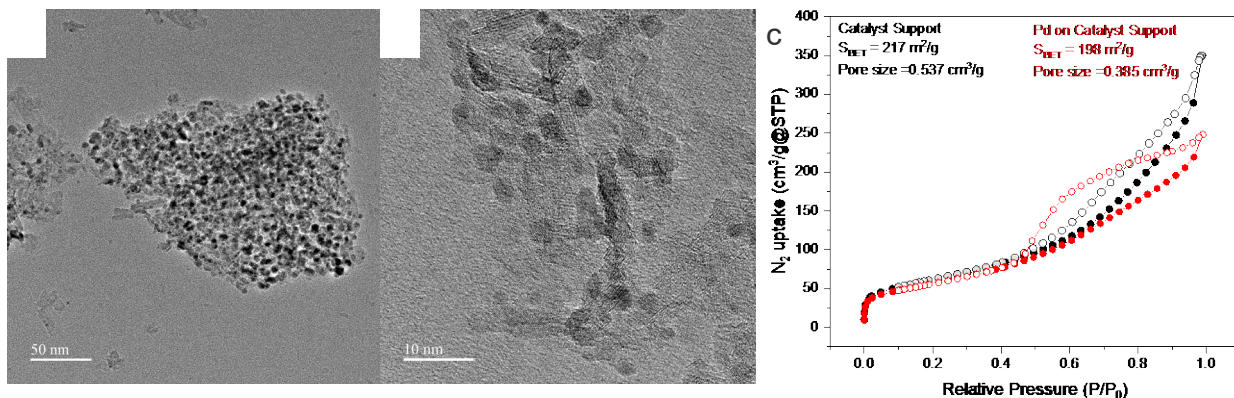


Figure 5. (a) low and (b) high magnification TEM images of Pd/MgO-Al₂O₃ catalyst. (c) BET surface area of MgO-Al₂O₃ catalyst with and without Pd.

Chemo selective hydrogenation of C=C bonds with these Pd-based bimetallic catalysts were studied using mesityl oxide as the substrate using high throughput batch reactor. Usage of high throughput reactor was beneficial to accelerate the activity study with numerous catalyst composition. All the activities reported herein corresponding to each catalyst was average of triplicate to minimize the error. Figure 6 shows the conversion of MO obtained after 10 min when the hydrogenation of mesityl oxide was carried out 40 °C using 45 psi of H₂ pressure. The activity comparison was made only after 10 min as longer reaction time resulted in complete conversion of mesityl oxide and prevent us to compare the activity among the different catalyst systems.

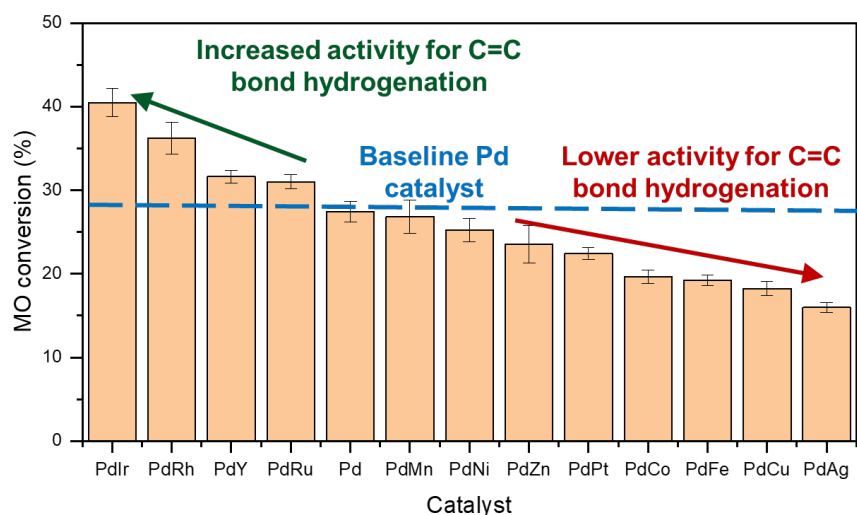
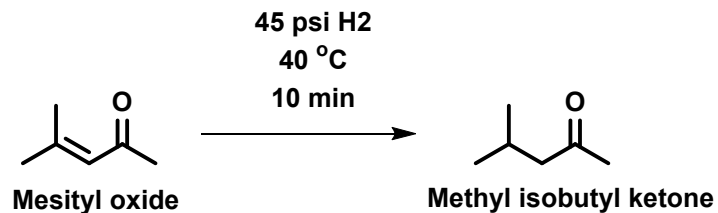


Figure 6. Activity of Pd-based bimetallic catalysts towards MO conversion which yielded MIBK as the sole product. Reaction condition: 20 wt% MO, 40 °C, 45 psi H₂.

It has been evident from the activity comparison that bimetallic catalysts such as PdRu, PdRh, PdIr and PdY resulted in higher catalytic activity compared to baseline Pd catalysts. The highest activity increment (1.3x) was noted with PdIr catalyst. Higher reactivity of Ru, Rh and Ir has been well documented in the hydrogenation literature and thus, we speculate that alloying with these metals led to higher activity compared to Pd catalyst. However, interestingly alloying with Pt did not result in increasing the activity despite Pt is known for its higher activity towards hydrogenation reaction. When 3d transition metals was used as the alloying element, catalytic activity was reduced compared to baseline Pd catalyst. Order of the catalytic activity obtained herein as follows Pd ~ PdMn > PdNi > PdZn > PdCo > PdFe. Although reduction of the catalytic activity was noted, the difference was not very significant, and we propose that effect of 3d transition metal alongside Pd has only marginal effect. Alloying with coinage metal such as Cu and Ag also resulted in reduction of catalytic activity. We next investigated the effect of hydrogen pressure during the C=C hydrogenation of MO. As shown in Figure 7, all the bimetallic catalysts show an increase in activity with the increase in hydrogen pressure irrespective of their corresponding baseline activity. The normalized activity of these catalysts was reported as mol of MIBK produced with respect to the Pd moles present in the catalyst. ~5-6 time increase in hydrogenation rate was obtained when pressure was increased from 45 to 270 psig. It is to be important note that even at highest pressure (270 psig) tested in this study none of the catalyst show any C=O hydrogenation of MO i.e., formation of methyl isobutyl carbinol (MIBC) further suggested that Pd based bimetallic catalysts tested herein are very selective towards C=C hydrogenation.

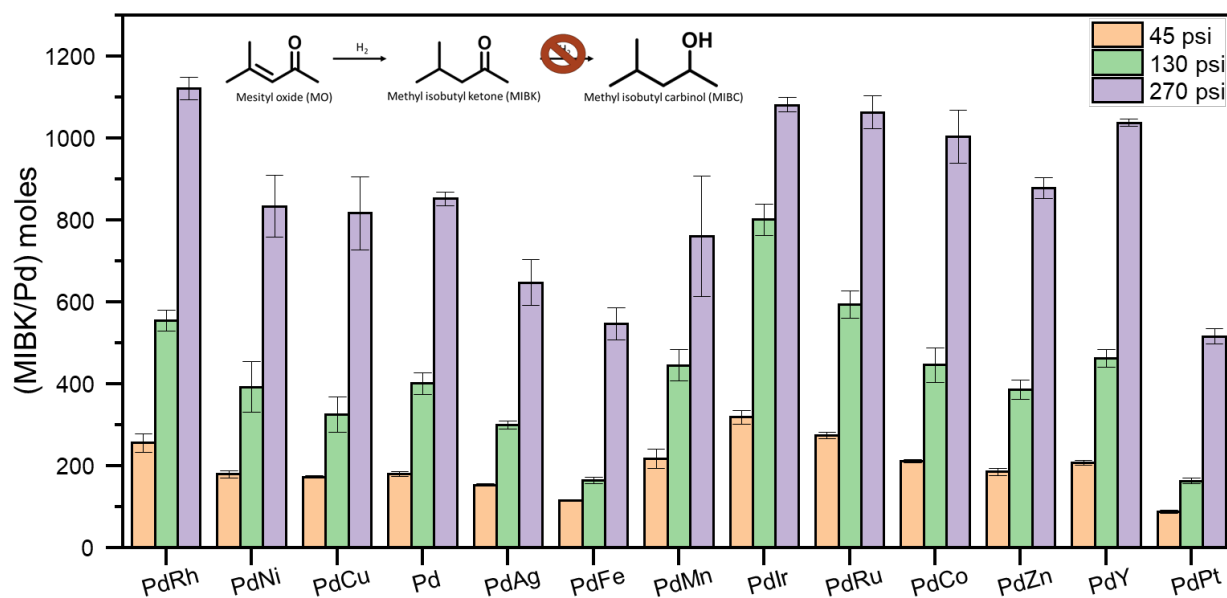


Figure 7. Activity of Pd-based bimetallic catalysts towards MO conversion at different hydrogen pressure. Reaction condition: 20 wt% MO, 40 °C, H₂ pressure 45-270 psi.

As none of the bimetallic catalysts show any activity towards C=O hydrogenation of α,β -unsaturated ketones, we next evaluated their activity towards C=O hydrogenation using 2-heptanone as the model substrate which only contain C=O functionality but devoid of any C=C functionality. When the 2-heptanone hydrogenation was carried out at 270 psig at 40 °C for 10 min, all the catalysts show their activity towards C=O hydrogenation albeit much lower activity was noted compared to C=C hydrogenation obtained as same reaction condition. Comparing the rate of MO (undergoes only C=C hydrogenation) and 2-heptanone (undergoes only C=O hydrogenation) hydrogenation shown in Figure 7 and 8 respectively, it is imperative that C=C

hydrogenation is much faster than C=O hydrogenation on all these catalysts. At the comparable condition such as at 270 psig H₂ pressure and at 40 °C, rate of C=C hydrogenation was nearly 3 orders of magnitude higher compared to C=O hydrogenation irrespective of the catalysts tested herein. Among the different Pd bimetallic catalysts tested herein, alloy catalysts containing PGM metals show higher activity compared to baseline Pd catalyst. The catalytic activity order obtained herein was PdIr < PdRu < PdPt < PdRh. While alloying with Pt did not show any beneficial activity increment in case of C=C hydrogenation, it shows significant effect during C=O hydrogenation as nearly an order of magnitude increase in hydrogenation rate was obtained with PdPt catalyst compared to Pd catalyst. Apart from PGM metals, alloying with Co and Ni with Pd also show an enhancement in hydrogenation rate, however, the effect was much smaller compared to the PGM metal. Although comparable activity towards 2-heptanone hydrogenation was apparent for PdCu, PdAg, PdZn, PdMn and PdFe catalyst with Pd catalyst, there might be a minor difference among these catalysts as shown in inset of Figure 8. While PdCu, PdAg and PdZn shows lower activity compared to Pd, PdMn and PdFe shows slightly higher activity.

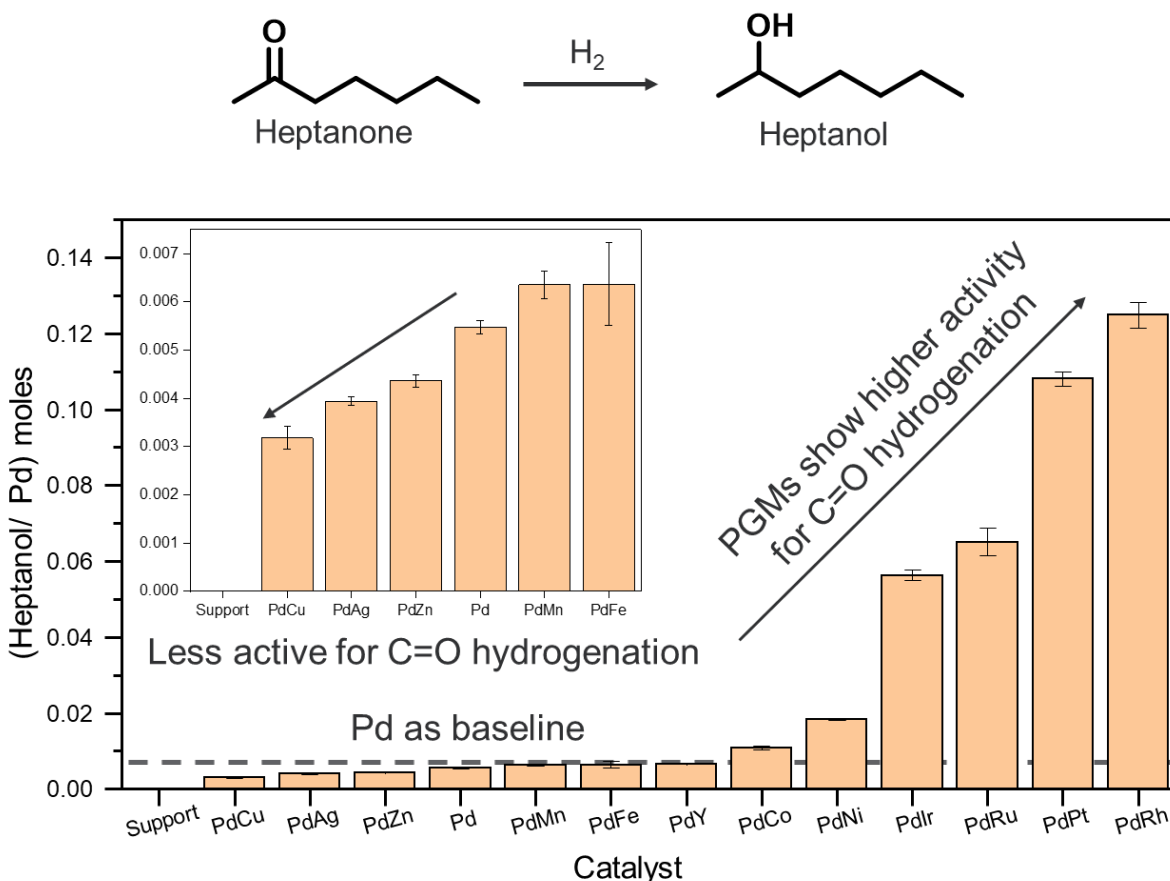


Figure 8. Activity of Pd-based bimetallic catalysts towards 2-heptanone hydrogenation. Reaction condition: 20 wt% MO, 40 °C, H₂ pressure 45-270 psi.

2-heptanone hydrogenation was also performed at different H₂ pressure such as 45, 130 and 270 psig. Hydrogenation rate was found to be increased with increasing pressure irrespective of catalyst composition. Thus, both C=C and C=O hydrogenation was found to be dependent on H₂ pressure and hydrogenation rate was increased with increasing hydrogen pressure. Surprisingly rate enhancement noted as a function of pressure was very similar in both C=C and C=O hydrogenation when MO and 2-heptanone was used as the substrate respectively.

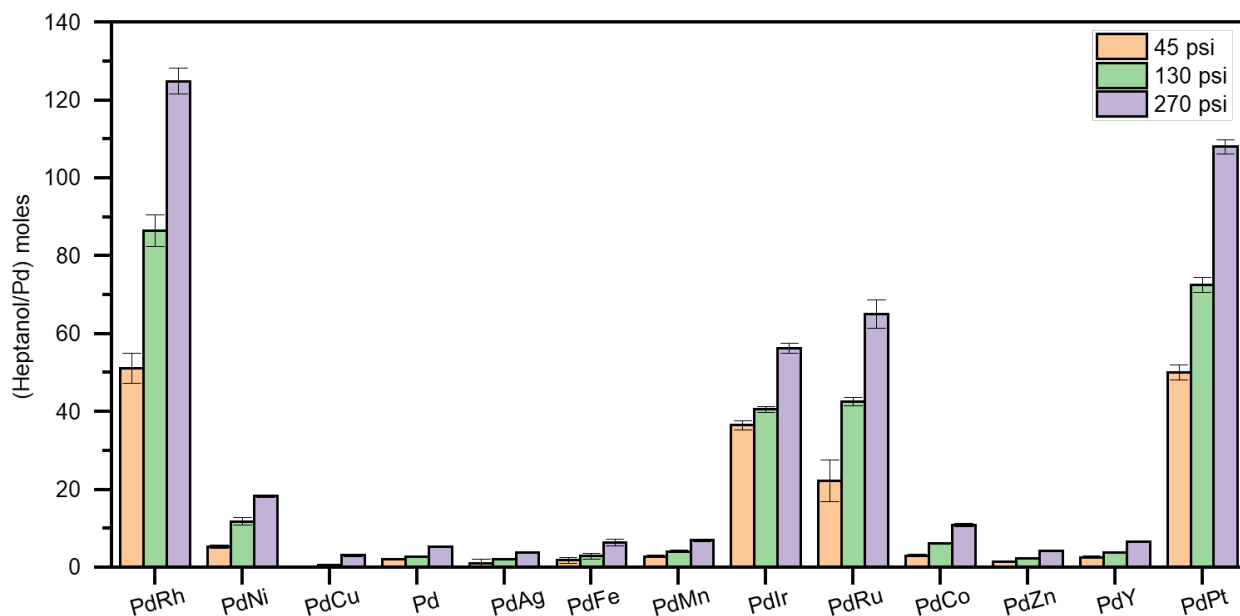


Figure 9. Activity of Pd-based bimetallic catalysts towards 2-heptanone hydrogenation at different hydrogen pressure. Reaction condition: 20 wt% MO, 40 °C, H₂ pressure 45-270 psi.

Figure 10 shows direct activity comparison of different Pd based bimetallic catalysts towards C=C and C=O hydrogenation using MO and 2-heptanone as the substrate at 130 psi at 40 °C. As mentioned earlier all the Pd based bimetallic catalysts shows much higher activity towards C=C hydrogenation compared to C=O hydrogenation indicated that activation energy of C=O hydrogenation is higher compared to C=C hydrogenation. At this condition, depending on the metal ~5-8 times higher activity was noted in case of C=C hydrogenation. It is also apparent that only those bimetallic catalyst containing PGM metals shows appreciable activity towards 2-heptanone hydrogenation.

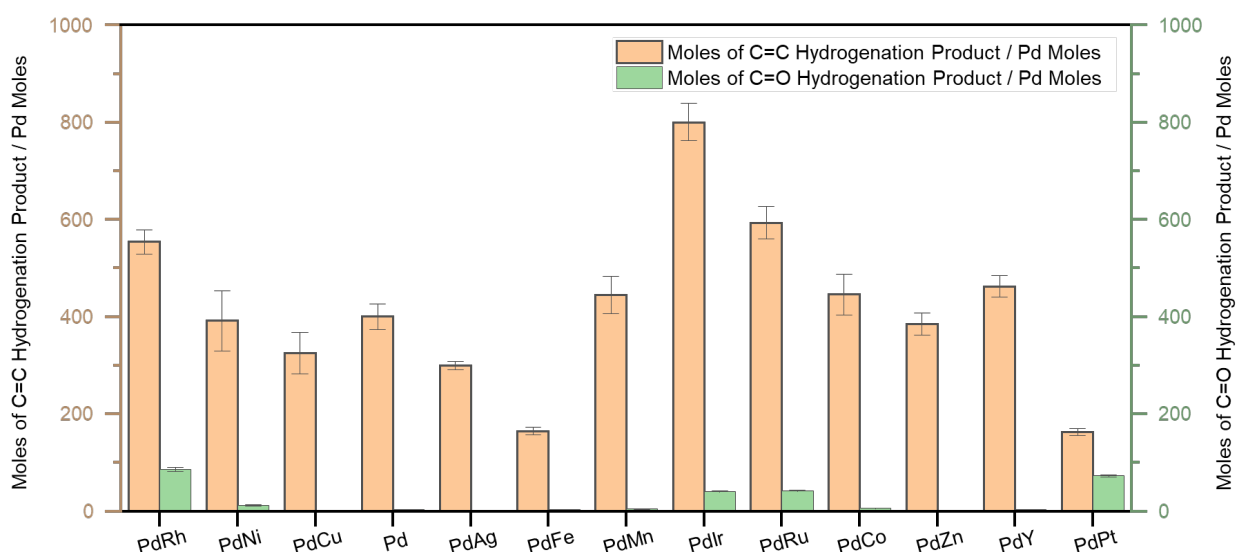


Figure 10. Comparison of activity among different Pd-based bimetallic catalysts during MO and 2-heptanone hydrogenation. Reaction condition: 20 wt% MO, 40 °C, H₂ pressure 130 psi.

Based on this screening study, we concluded that choice of Ru and Rh as an alloying metal with Pd have significant impact on both C=O and C=C hydrogenation though former (10x enhancement in C=O hydrogenation activity) was more impacted than later (5x enhancement in C=C hydrogenation). On the other hand, PdZn shows comparable activity to Pd catalyst for C=C hydrogenation, however, a decrease in C=O hydrogenation was noted towards C=O hydrogenation, thus fulfilled the criteria for our catalyst design during ketone condensation steps as shown in Figure 2. We then selected PdZn as our optimum catalyst and studied their activity towards CO tolerance. During ketone synthesis reaction, we have noted the formation of PdZn phase improved the stability of the catalyst in presence of ppm level CO whereas Pd catalyst undergoes severe deactivation at the same condition. We hypothesized that weaker CO binding to PdZn alloy phase did not result in deactivation of catalyst. To delineate the higher CO tolerance of PdZn catalyst we have performed electrochemical CO stripping experiment. As MgO-Al₂O₃ is nonconductive we prepared both Pd and PdZn catalyst using Vulcan carbon as the support materials.

Figure 11a shows electrochemical CO stripping of PdZn catalyst which shows a peak at 0.8 V corresponding to CO stripping at the anodic branch of the spectrum. Figure 11b shows the comparison of the CO stripping peak obtained with Pd and PdZn catalyst. Lower onset potential associated with PdZn compared to Pd suggested that lower energy is required to break the metal-CO bond further established the weaker bonding of CO on PdZn alloy surface compared to pristine Pd. This data unambiguously confirmed the benefits of using PdZn catalyst as opposed to Pd catalyst during ketone condensation reaction as it provides higher CO tolerance.

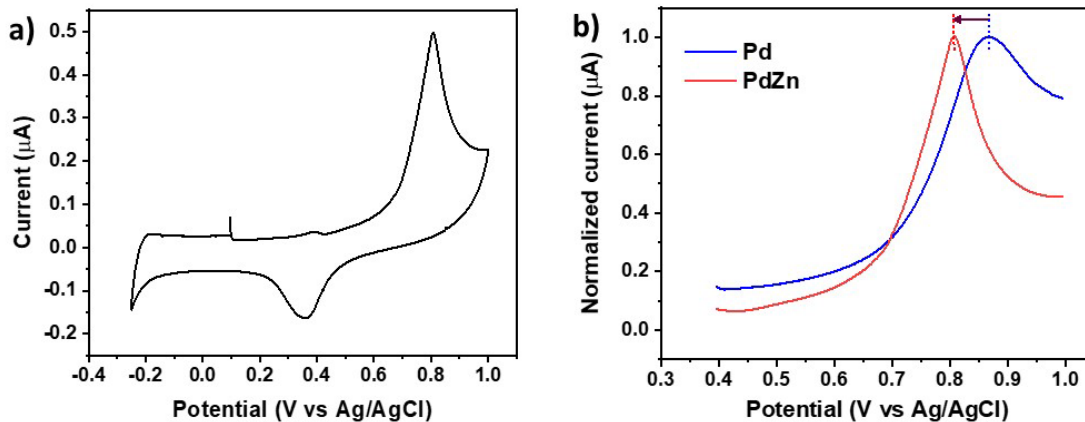


Figure 11. (a) Electrochemical CO stripping spectrum of PdZn/C catalyst. (b) comparison of CO stripping peak among Pd and PdZn catalyst.

4.0 Conclusion

In conclusion, we have synthesized a series of Pd based bimetallic catalysts with different alloying elements in order to optimize a catalyst during ketone condensation reaction of the overall ethanol to SAF process. Catalysts were synthesized using incipient wet impregnation technique to deposit the metallic phase on the MgO-Al₂O₃ surface. Catalysts were characterized by powder XRD technique which shows suggested the formation of bimetallic particles. Activity of these catalysts were evaluated towards C=C and C=O hydrogenation using mesityl oxide and 2-heptanone as the model substrate. All the Pd based bimetallic catalysts prepared herein shows much higher activity towards C=C hydrogenation compared to C=O hydrogenation further highlight the usage of Pd based catalyst for the ketone condensation reaction. Performance evaluation of these catalysts shows that PdRu, PdRh and PdIr could be a viable choice as the highest rate enhancement during C=C hydrogenation was noted, however, controlled studies suggested these catalysts also enhance the C=O hydrogenation. Moreover, the higher cost of Rh, Ru or Ir is also not viable industrially as it significantly increases the catalyst cost. We have identified PdZn as one of the potential catalyst due to its comparable activity towards C=C hydrogenation whereas reduced activity towards C=O hydrogenation compared to baseline Pd catalyst. Thus, PdZn catalyst fulfills the criteria of our catalyst design. Moreover, due to weaker CO binding to PdZn catalyst it further provides the benefits of higher CO tolerance.

By leveraging the PNNL high throughput catalyst testing facility we were able to screen numerous amount Pd based bimetallic catalyst and gained an understanding about their corresponding activity towards chemo selective C=C hydrogenation. While the catalyst system for both ketone synthesis and hydrodeoxygenation was already matured, this LDRD funding was critical for us to identify the optimized catalyst system for the ketone condensation steps and address the technological gap present in the overall process.

5.0 Reference

1. Dagle, R.A.; Winkelman, A. D.; Ramasamy, K. K.; Dagle, V. L.; Weber, R. S. *Ind. Eng. Chem. Res.* **2020**, 59, 4843.
2. Abdulrazzaq, H. T.; Schwartz, T. J. 10.1016/B978-0-12-811458-2.12001-2.
3. Ramasamy, K. K.; Guo, M. F.; Gray, M.; Subramaniam, S.; Alvarez-Vasco, C. US Patent No. 10, 221, 119
4. Ramasamy, K. K.; Guo, M. F.; Subramaniam, S.; Sanyal, U.; Brady, C. O. US 2021/0269377A1
5. Subramaniam, S.; Guo, M. F.; Bathena, T.; Gray, M.; Zhang, X.; Martinez, A. I.; Kovarik, L.; Goulas, K. A.; Ramasamy, K. K. *Angew. Chem. Int. Ed.* **2020**, 59, 2-10.
6. Sheng, X; Li, N.; Li, G.; Wang, W, Wang, A.; Cong, C.; Wang, X.; Zhang, T. *Green Chem.* **2016**, 18, 3707.

Pacific Northwest National Laboratory

902 Battelle Boulevard
P.O. Box 999
Richland, WA 99354

1-888-375-PNNL (7665)

www.pnnl.gov